Eur Biophys J (1996) 24: 359–370

ARTICLE

M. Canepari · M. Campani · L. Spadavecchia
V. Torre

CCD imaging of the electrical activity in the leech nervous system

Received: 3 January 1996 / Accepted: 24 April 1996

Abstract A single ganglion of the nervous system of the leech *Hirudo medicinalis* was isolated. One or both roots emerging from each side of the ganglion were sucked into suction pipettes used either for extracellular stimulation or for recording the gross electrical activity. The ganglion was stained with the fluorescence voltage sensitive dye Di-4-Anepps. The fluorescence was measured with a nitrogen cooled CCD camera. Our recording system allowed us to measure in real time slow optical signals corresponding to changes in light intensity of at least 5‰. These signals were caused by the direct polarization of neuronal structures, the afterhyperpolarization or the afterdischarge induced by a prolonged stimulation. When images were acquired at fixed times, several of them could be averaged and optical signals of at least 2‰ could be reliably measured. These optical signals originated from well identified neurons, such as T, P and N sensory neurons. By taking images at different times and at different focal planes, electrical events could be followed at a temporal resolution of 50 Hz. The three dimensional dynamics of electrical events, initiated by a specific stimulation, was imaged and the spread of excitation among leech neurons was followed. When two roots were selectively stimulated, their neuronal interactions could be imaged and the linear and non-linear terms of the interaction could be characterized.

Key words Voltage-sensitive dyes · Fluorescence · Leech

M. Canepari · M. Campani · V. Torre
I.N.F.M. Via dell'Acciaio, I-16146 Genova, Italy

L. Spadavecchia
Istituto di Cibernetica e Biofisica, C.N.R., Via De Marini, I-16146 Genova, Italy

V. Torre (✉)
Dipartimento di Fisica, Universita' di Genova, Via Dodecaneso 33, I-16146 Genova, Italy
(Tel. and Fax No. +39-10-3536311, e-mail: torre@genova.infn.it)

Introduction

The analysis of the integrative properties and the information processing of the nervous system requires the study of electrical events originating from different locations of the neuronal network and occurring with different time courses. Therefore, in order to understand the workings of the central nervous system, it is necessary to detect electrical signals at a very precise temporal and spatial resolution. Such a comprehensive description is at present beyond available experimental techniques, but certain practicable approaches are available. In several instances, when a nervous system is analysed as a whole, a more compact description may be useful, in which the information is averaged both in space and time. When the integrative properties of a small nervous system, such as that of many invertebrate animals, are analysed, a coarse analysis may be adequate and provide useful information. One possibility is to use optical recording techniques (Cohen and Salzberg 1975; Grinvald 1985; Gross et al. 1986; Fromherz and Lambacher 1991; Wu and Cohen 1992) so that the electrical signal can be detected at a variable spatial and temporal resolution. Optical signals produced by voltage sensitive dyes are usually detected with photodiodes, arranged in a suitable matrix with a maximal resolution of about 20×20 elements (Wu and Cohen 1992), but with a temporal resolution in the kHz range. CCD cameras have been used to detect slow intrinsic signals associated with metabolic changes induced by the electrical activity (Grinvald et al. 1986) and to measure fluorescence changes of voltage sensitive dyes caused by slow electrical waves (Kauer 1988; Delaney et al. 1994). In all these experiments the neurons originating the optical signals could not be identified.

In this paper we describe some preliminary experiments performed in the nervous system of the leech *Hirudo medicinalis* (Muller et al. 1981) with a commercially available CCD camera. Optical recordings with voltage sensitive dyes from the leech neurons with photodiodes have already been described by Salzberg et al. (1973) and by Grinvald

et al. (1987). Isolated leech ganglia were incubated with the voltage sensitive dye Di-4-Anepps whose fluorescence depends on the membrane potential of stained neurons. The fluorescence was measured with a nitrogen cooled CCD camera. The CCD camera was used in two different modes. In the first mode, image sequences were acquired in real time and the CCD camera was able to acquire and transfer an image of 27×38 pixels at about 5 Hz. In this mode optical signals could be observed, originating from the ganglion, either due to a direct polarization of the neurons or an afterdischarge or an afterhyperpolarization of viewed neurons. These signals were caused by changes of fluorescence of about 5‰ or more. In the second mode, images were taken at fixed times, so that they could be averaged over different trials. In this mode optical signals were detected, originating from the cell body of well identified neurons and caused by one or a few action potentials occurring in the imaged neurons. The amplitude of optical signals which could be detected with this mode was as low as 2‰. By taking images at different times and focal planes, a coarse three dimensional dynamic description of the electrical events was obtained and an effective time resolution of 50 Hz was achieved.

These results indicate that a CCD camera can be used to detect the excitation of well identified neurons at a moderate time resolution, i.e. at about 50 Hz and to obtain useful information for the understanding of the dynamics of a neuronal network.

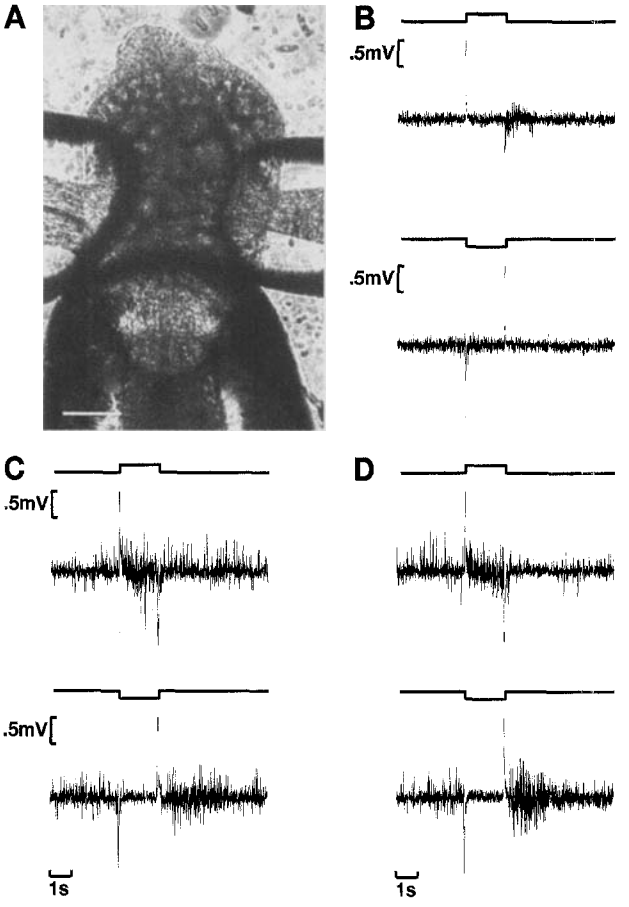

Fig. 1A–D The isolated leech ganglion used in the experiments. **A** A CCD image in transmitted light at full resolution (416×578 pixels) of an isolated leech ganglion, with the two pairs of roots and a bundle of connective fibers sucked into three suction electrodes. 16×objective. The calibration bar indicates 150 μm. **B** Extracellular recordings from the left roots following the stimulation of the connective fibers with extracellular voltage pulses of opposite polarities applied through the suction electrode. **C** and **D** Extracellular recordings from the connective fibers following the stimulation of the *left* (**C**) and *right* (**D**) pairs of roots with extracellular voltage pulses of opposite polarities applied through the suction electrode. In **B**, **C** and **D** the solid line is the artifact of the applied extracellular stimulation. The intensity of the voltage pulse was 1 V

Materials and methods

Preparation and electrical recordings

Experiments were performed on the leech *Hirudo medicinalis*, collected in ponds of central Italy or provided by Ricarimpex (Eysines, France). A single ganglion of the nervous system of the leech was isolated. The isolated ganglion was one between ganglion 7 and 18 (see Muller et al. 1981). In some experiments one or two roots from each side of the ganglion and a bundle of connective fibers were sucked into suction electrodes, as shown in Fig. 1A. In other experiments, the left anterior and posterior roots were sucked into two different suction electrodes and the third suction pipette was either used to record the electrical activity from the connective fibers or pressed against the ganglion so as to reduce the distance between the microscope objectives and the viewed neurons. The isolated ganglion was placed in a perfusion chamber mounted on the stage of an inverted microscope (ZEISS IM 35).

Figure 1B illustrates extracellular voltage recordings from the right pair of roots of the ganglion of Fig. 1A, following the stimulation of the connective fibers with a voltage pulse of 2 s with a positive (upper trace) and negative (lower trace) polarity. The electrical activity in the absence of stimulation was very reduced and activated only at the cessation of the positive voltage and during the negative voltage. Different behaviour was observed when the roots were stimulated and the electrical activity was recorded from the connective fibers (see Fig. 1C, D). In this case there was a vigorous spontaneous activity which was enhanced by applying positive pulses and drastically reduced with negative pulses. At the cessation of the stimulation of the right pair of roots (see Fig. 1D), the spontaneous activity decreased following a positive pulse and increased following a negative pulse. A similar, but not identical behaviour was observed by stimulating the left pair of roots (see Fig. 1C). The differences between the stimulation of the two pairs of roots were most likely caused by a different electrical contact established by the two suction electrodes. These effects were graded with the amplitude of the voltage pulse applied. When one root was stimulated with a much weaker voltage pulse (i.e. between 0.05 and 0.2 V)

single extracellular action potentials could be recovered (see Figs. 4–7) from the other ipsilateral root. Ganglia were incubated in a saline medium (110 mM NaCl, 2.5 mM KCl, 8 mM CaCl, 1.5 mM MgCl, buffered to pH 7.6 with 10 mM HEPES and NaOH) containing the fluorescent dye. The dye Di-4-Anepps (Molecular Probes) was used. The dye was dissolved in ethanol and heated at 50 °C for 30 min; in many cases pluronic acid F-127 (Molecular Probes) was also added. The final concentration of the dye used to stain the ganglia ranged between 0.2 and 1 mg/ml and the incubation time varied between 20 and 60 min. During incubation the electrical activity of the ganglion was monitored by stimulating one root with a voltage pulse and recording the extracellular voltage response from the connective fibers. Usually, the electrical activity before and after dye incubation was almost the same; if not, the experiment was abandoned. After incubation the ganglia were rinsed several times in the usual saline medium. The experiments were performed at a room temperature varying between 18 ° and 25 °C.

Optical recordings

The exciting light was provided by a tungsten lamp (Philips GCS AI/216) or a mercury lamp (Osram HBO 100 W/2) placed at the back of the microscope and illuminating the preparation through the objectives. A good stability of the lamp was obtained by carefully selecting the bulb to be used. The wavelength of the exciting light was selected at 498 nm with a narrow band interference filter. A dichroic mirror was used, (Texas red ZEISS) transmitting at 515 nm and reflecting at 501 nm. The fluorescence was measured at 610 nm with another narrow band filter (3 nm bandwidth). The fluorescence light could be either monitored with a single photodiode (OSD 100-5T Centronic) or diverted to the CCD camera, through a side port of the microscope. As shown by Fromherz and Lambacher (1991) in leech neurons, a decrease of fluorescence of the dye Di-4-Anepps of 10% at the measured wavelength indicates a membrane depolarization of about 100 mV; similarly, an increase of fluorescence of 10% indicates a membrane hyperpolarization of about 100 mV. The objectives of the microscope had a magnification of ×16 (N.A. 0.8) or ×25 (N.A. 0.6 working distance 1.67 mm). A nitrogen cooled CCD camera was used (Astromed CCD 3200 Imaging system using a CCD P8600 series from EEV Ltd. England with a quantum efficiency of about 50% with peak dark current ~0.1 electron/sec and a readout noise of about 150 electrons). The imaging system was able to digitize each image with a resolution of 16 bits. The time required to digitize and transfer a full image of 416×578 pixels was more than 1 second. In the presence of a stable light source and when the dark current of each light sensor was drastically reduced by cooling at the temperature of liquid nitrogen, the major source of noise was photon noise (Wu & Cohen 1992). When N photons are absorbed by the sensor, the noise N, i.e. the standard deviation of fluctuations, is in the order of $\sqrt{N}$. As a consequence, in order to have a signal to noise ratio (S/N) of at least 500, it is necessary to have signals corresponding to at least 250 000 absorbed photons. However the system was not able to measure a number of photons larger than about 1 300 000 photons/pixel in one frame. In order to increase the temporal resolution of the imaging system, a binning of the image was found convenient. Since the number of photons that could be measured by a single pixel was always limited, this procedure of space integration was also used to increase the S/N. Images were binned by a factor between 5 and 15, so that the final resolution of each image ranged between 27×38 and 82×115 pixels. With this arrangement the temporal resolution (i.e. the acquisition frequency) varied between 3 and 5 Hz. The exposure times was 20 ms and was controlled by a shutter (Vincent Associates) and the readout time was equal to $\frac{1}{f}$-exposure time, where f is the acquisition frequency. When a stable electrical signal was observed, an experiment was started and a full CCD image of the viewed ganglion acquired. Images were acquired in two different modes, referred to as "real time" and "fixed time".

Image analysis

Images taken before stimulation were averaged and used as the baseline fluorescence F_b. The fluorescence signal S_i related to the electrical activity is the fractional fluorescence change computed as:

$$S_i = \frac{F_i - F_b}{F_b} \quad (1)$$

where F_i is the fluorescence of image i. Using this procedure for each image sequence, a set of signal images S_i could be obtained. Fractional fluorescence changes are indicated in false colors according to the table reproduced in each Figure. Signal images were often smoothed by the convolution with an appropriate filter, usually a symmetrical Gaussian function. A bleaching larger than 3‰ was only rarely observed over the duration of a recording (3–5 seconds). In these cases images were digitally corrected for the loss of intensity caused by the bleaching.

Noise and bleaching

The amount of bleaching and noise of the imaging system was evaluated by analysing the data shown in Fig. 2. In this test, 60 images of a stained ganglion were acquired with a 15×15 binning corresponding to images of 27×38 pixels. Figure 2A shows the number of photons collected by one pixel. Because of the presence of dye bleaching, the average number of detected photons decreased with time. In order to estimate the bleaching for a single pixel, for a region of 10×10 and for the entire image of 27×38 pixels, we evaluated either a linear bleaching, corresponding to:

$$I = at + b \quad (2)$$

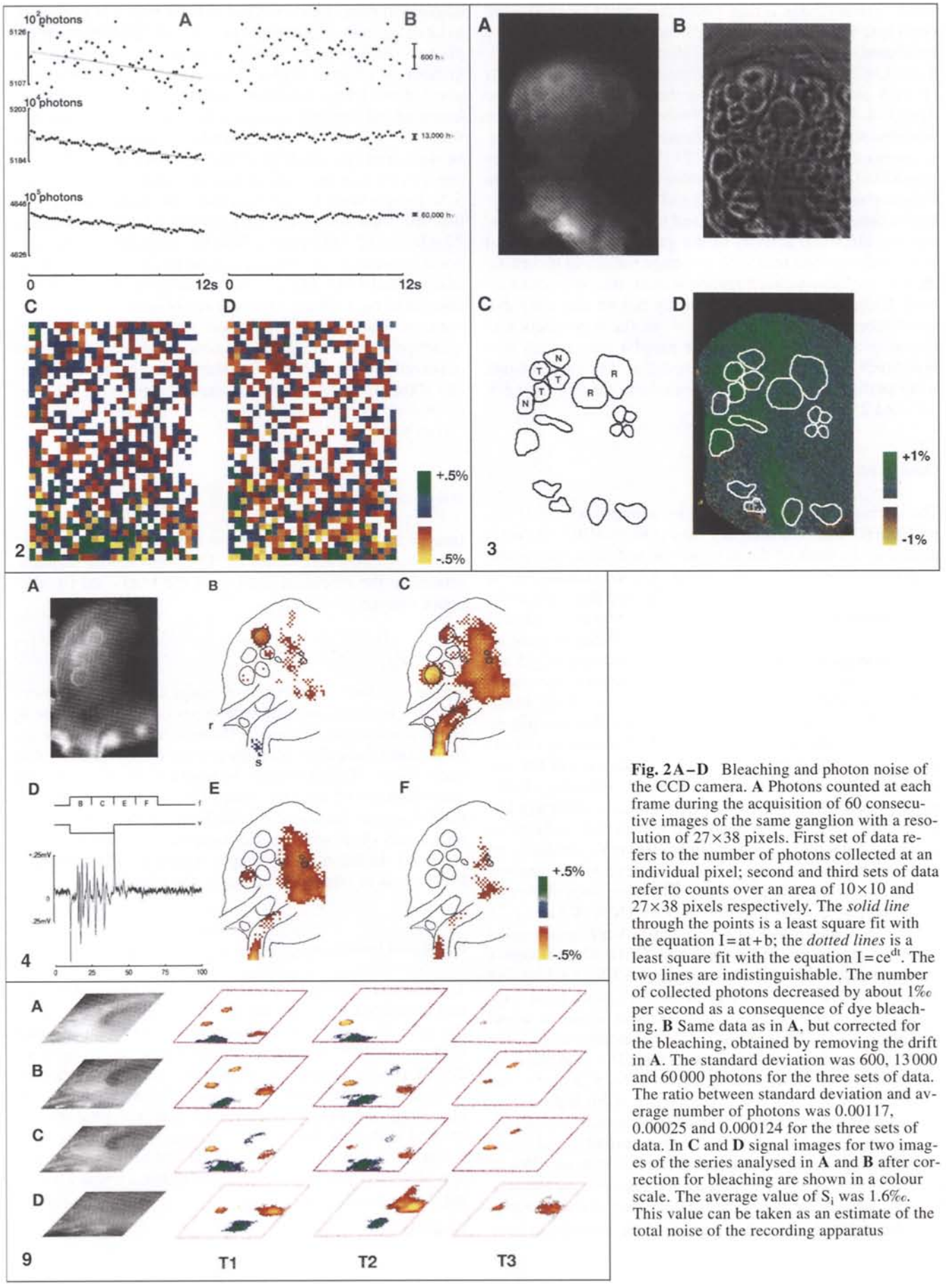

Fig. 2A–D Bleaching and photon noise of the CCD camera. **A** Photons counted at each frame during the acquisition of 60 consecutive images of the same ganglion with a resolution of 27×38 pixels. First set of data refers to the number of photons collected at an individual pixel; second and third sets of data refer to counts over an area of 10×10 and 27×38 pixels respectively. The *solid line* through the points is a least square fit with the equation $I = at + b$; the *dotted lines* is a least square fit with the equation $I = ce^{dt}$. The two lines are indistinguishable. The number of collected photons decreased by about 1‰ per second as a consequence of dye bleaching. **B** Same data as in **A**, but corrected for the bleaching, obtained by removing the drift in **A**. The standard deviation was 600, 13000 and 60000 photons for the three sets of data. The ratio between standard deviation and average number of photons was 0.00117, 0.00025 and 0.000124 for the three sets of data. In **C** and **D** signal images for two images of the series analysed in **A** and **B** after correction for bleaching are shown in a colour scale. The average value of S_i was 1.6‰. This value can be taken as an estimate of the total noise of the recording apparatus

where I is the number of collected photons, t is the time and a and b are parameters to be estimated, or an exponential decline, corresponding to:

$$I = ce^{td} \quad (3)$$

A best fit with these two equations to the data shown in Fig. 2 A provides the values of a = –52624, = 484 107 840, c = b and d = –0.00011 for the full image of 27×38 pixels. The linear bleaching (dotted line) or an exponential bleaching (continuous line) provided almost indistinguishable fits of the experimental data. Similar results were obtained when photons were counted over an area corresponding to 10×10 pixels (middle data in A) or over the entire image (lower data in A). The decline of the number of detected photons, caused by bleaching, was compensated by appropriately multiplying the measured number of photons (see Fig. 2B). The standard deviation was 600, 13 000 and 60 000 photons for the three sets of data. The ratio between standard deviation and average number of photons was 0.00117, 0.00025 and 0.000124 for the three sets of data. These results indicate that the effect of bleaching is about 1‰ per second and can be effectively corrected and that the total noise in photon counting approaches the limit set by photon noise which is expected to be $\frac{\sqrt{N}}{N}$. This ratio is 0.0014, 0.000138 and 0.0000456 for the three sets of data shown in A and B. A comparison between these values and those measured indicates that the noise in our imaging device is close to photon noise. C and D show signal images S_i for two images of the series analysed in A and B. This ratio is displayed in the colour scale shown in the right lower corner. The average value of S_i was 1.6‰ and could be taken as an estimate of the noise in real time mode. In order to detect smaller signals, it was necessary to acquire images in "fixed time" mode. In this mode, by averaging at least 10 images, fluorescence changes as small as 2‰ could be reliably detected.

Real time mode

In this mode of operation, image sequences (from 20 to 30 images) were taken at a reduced spatial resolution; each image sequence contained from 3 to 7 images taken before the voltage stimulation and from 15 to 25 images taken during and following the stimulation. In this mode the exact timing of image acquisition was not controlled, but could be determined by measuring the artifact of the T.V. camera shutter and optical signals larger than 5‰ could be reliably detected (see Fig. 7).

Fixed time mode

The total noise of our imaging system, operating in "real time" is greater than 1.6‰ of the total light measured. The shortest shutter opening, which could be achieved by our imaging system, is of the order of 18–20 msec. Assuming that the dye Di-4-Anepps provides a signal of 10% for a change of 100 mV in the membrane potential (Fromherz and Lambacher 1991), the occurrence of a spike of a duration of 1 or 2 msec will produce a signal not larger than 1%. As the light collected at a pixel does not come only from the imaged neuron but also from other non-excitable stained structures, the optical signal caused by the firing of a single action potential is more likely to be only some ‰. As a consequence, in order to detect images of a single spike the background noise had to be reduced to less than 1‰. This could be obtained by averaging images over several runs, which was possible in the "fixed time" mode. In this mode two images were acquired in each run; the first image before the stimulation (used as the baseline fluorescence F_b) and the second image at a fixed time after the onset of the stimulation. This procedure was usually repeated 10 times. Images taken at the same fixed time and with the same time exposure of 20 ms were averaged. This was possible when the electrical signal was identical over the different trials to be averaged. Within the exposure time window the number of spines elicited by one electrical stimulation was usually constant. As a consequence, in fixed time mode an effective increase of the S/N was obtained and optical signals as low as 2‰ could be reliably detected. This allowed the detection of optical signals caused by action potentials occurring in the viewed neurons. The timing of the acquisition of the second image was varied, so that it was possible to have images of the electrical activity every 10 or 20 msec (see Fig. 4).

Fig. 3A–D The localization of optical signals. **A** A CCD image of the fluorescence from the stained ganglion at full resolution (416×578 pixels). The ventral side of the ganglion was focused and the posterior connective was sucked into a suction pipette. The calibration bar indicates 150 µm. **B** The image of **A** after the processing with suitable contrast enhancement procedures. **C**: Some neuronal profiles extracted from **B**. 2 Retzius cells are indicated by R, 3 touch neurons by T and 2 noxious neurons by N. **D** The neuronal map shown in **C** superimposed to a signal image obtained during the stimulation with a voltage pulse of 3 V lasting for 500 msec. Each image was obtained with an exposure of 18 ms, with a binning of 5, leading to images of 82×115 pixels. 25×objective, N.A. 0.6

Fig. 4A–F Imaging the electrical activity of identified neurons. **A** is a full image of the viewed ganglion. **B, C, E** and **F** are optical signals obtained at the times indicated by the corresponding letter in **D**. Images taken in "fixed time" mode (see Method section) and 10 runs were used to obtain one optical signal. Signal images taken with a binning of 8, leading to images of 52×72 pixels, 25×objectives, N.A. 0.6. D: Extracellular recording from the anterior left root (*R*) following the stimulation of the posterior left root (*S*) with a voltage step of 0.1 V. The line indicated by v is the stimulus artifact, the line indicated by f is shutter artifact and the letters indicate the timing of shutter openings

Fig. 9A–D Three dimensional reconstruction of the dynamics of the electrical activity. **A, B, C** and **D** reproduce four fluoresence images of the ganglion taken by focussing the superficial ventral layer and three other more interior layers. The second, third and fourth column reproduce signal images taken at the corresponding focal planes as in the first column. T_1, T_2 and T_3 were acquired 0,20 ms and 40 ms after the onset of the stimulation respectively

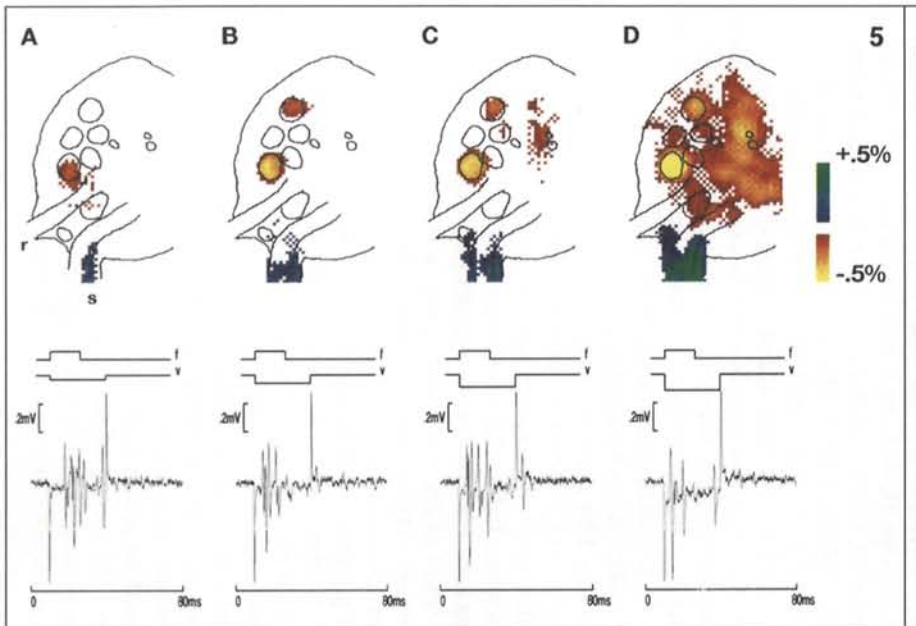
A
B
C
D
5
r
s
+.5%
-.5%
f
v
2mV
0
80ms

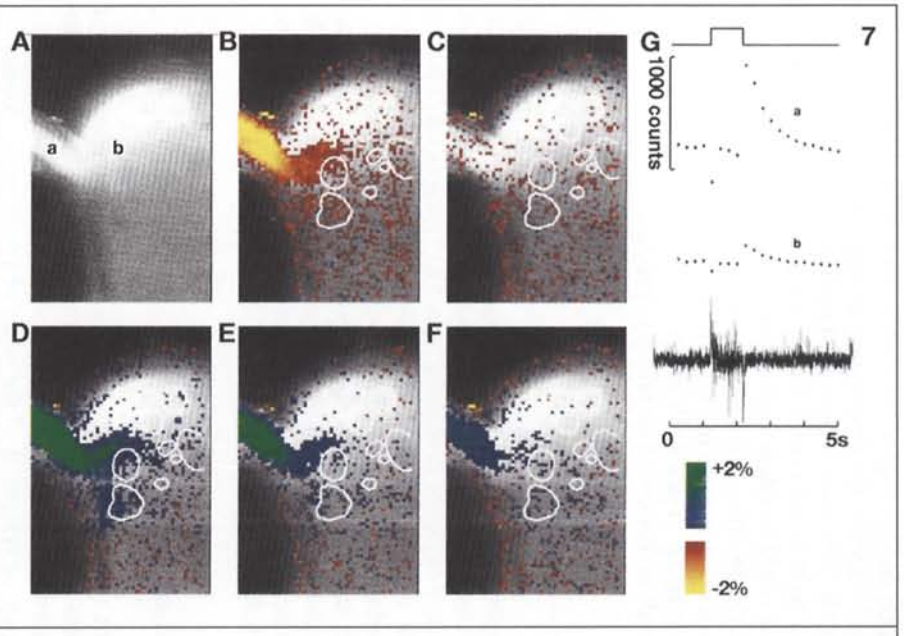
A
B
C
D
E
F
G
7
a
b
1000 counts
0
5s
+2%
-2%

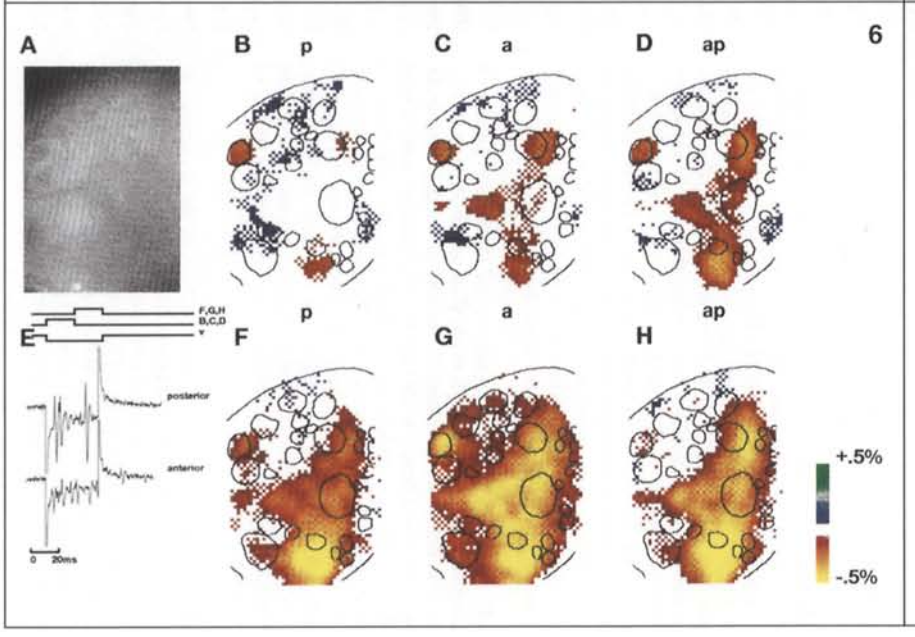
A
B p
C a
D ap
6
p
a
ap
E
F,G,H
B,C,D
posterior
anterior
0
20ms
F
G
H
+.5%
-.5%

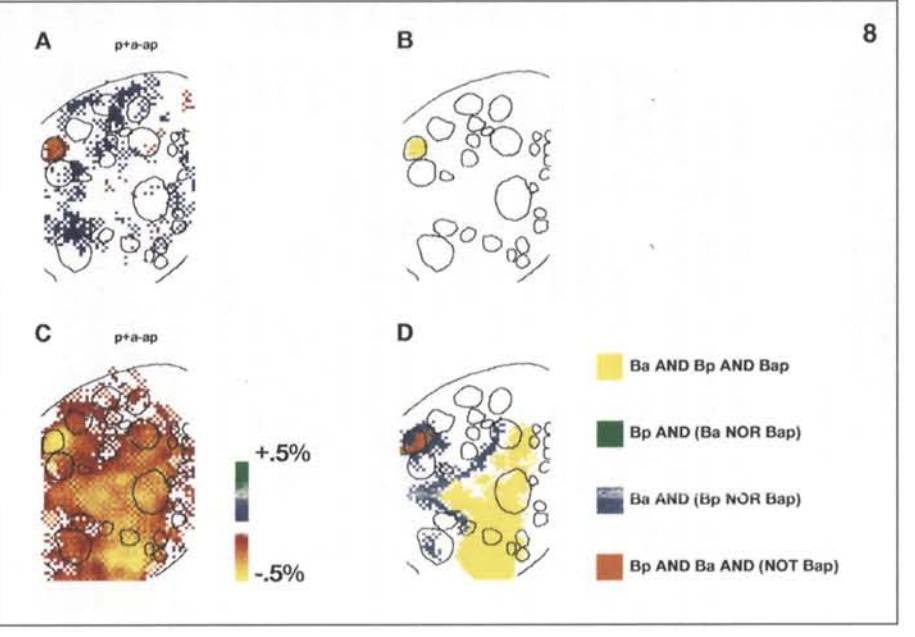
A p+a-ap
B
8
C p+a-ap
D
+.5%
-.5%
Ba AND Bp AND Bap
Bp AND (Ba NOR Bap)
Ba AND (Bp NOR Bap)
Bp AND Ba AND (NOT Bap)

Localization of optical signals

When the stimulation of the roots caused an evident electrical signal (see Fig. 1), fluorescence image were taken during the electrical stimulation.

Figure 3A illustrates a fluorescence image of the ganglion taken by the CCD camera at the full resolution of 416×578. Some neurons are clearly visible and can be identified in the atlas of the leech nervous system (Muller et al. 1981). Figure 3D reproduces signal images in a color scale (see right lower corner), obtained by the application to the suction electrode of a voltage pulse of 3 V to the left side roots. The stimulation induced a clear increase of fluorescence (indicated in blue and green). Decreasing the pulse amplitude produced less diffuse and intense optical signal indicating a less pronounced membrane hyperpolarization. The image shown in Fig. 3 A was printed on a laser printer which compressed the image to 6 bits, thus leading to an evident degradation of the visibility of the underlying neuronal structure. When the original image was processed by suitable contrast enhancement procedures, the image shown in Fig. 3B could be obtained, where many more neuronal structures were visible. By a semiautomatic procedure, the neuronal map shown in Fig. 3C was obtained from this image. In this map several well known neurons of the leech ganglion can be identified. Those labelled with R are Retzius cells, and those labelled with N and T are sensory neurons specific for noxious and touch stimuli. When the neuronal map of Fig. 3C is superimposed on the signal image of Fig. 3D, the neurons from which a clear optical signal was detected can be immediately identified as two T cells. As the preparation was viewed with a normal microscope and not with a confocal microscope, the light collected by the imaging device originated from sections of the preparation with different widths. In order to evaluate the accuracy of the localization in depth of our fluorescence signals, the preparation was viewed at different focal planes. The fluorescence signal had well defined boundaries when viewed neurons were in focus and deteriorated when they were out of focus.

Fig. 5A–D Imaging electrical signals of increasing intensity. Lower row reproduces extracellular recording from the left anterior root (*R*) following the stimulation of the left posterior root (*S*) with a voltage step of increasing intensities of 0.075 (**A**), 0.1 (**B**), 0.125 (**C**) and 0.25 (**D**). The stimulus artifact is indicated by the letter v. Upper column reproduces the optical signals obtained during the corresponding stimulations at the time indicated by the shutter artifact (*f*). Each optical signal was obtained as the average of 10 different trials. Signal images taken with a binning of 8, leading to images of 52×72 pixels, 25×objectives, N.A. 0.6

Fig. 6A–H Imaging the interaction of two different inputs. **A** The full image of the ganglion. Signal images taken with a binning of 8, leading to images of 52×72 pixels, 25×objectives, N.A. 0.6. **B, C** and **D** Optical signals obtained by the stimulation of the left posterior (**B**), left anterior (**C**) and both left roots (**D**) with a voltage pulse of 0.175 V. Images taken in "fixed time" mode at the time indicated by the shutter artifact shown in **E**. **F, G** and **H** as in **B, C** and **D** but images taken at the time indicated by the shutter artifact shown in **G**. Images were averaged over 10 different runs. **E** reproduces the stimulus artifact (*v*), the shutter artifact corresponding to the acquisition of images in **A, B** and **C** and those in **D, E** and **F**. The electrical response recorded from the left posterior and anterior root are also shown in **E**

Fig. 7A–F CCD imges in real time during the stimulation of a root with a depolarizing voltage pulse. **A** A fluorescence image of the ventral side of a ganglion. The stimulus was a depolarizing voltage pulse of V lasting for 1 second. **B, C, D, E** and **F** are signal images S_i coded as in the color scale in the right lower corner, superimposed to the image shown in **A** and the neuronal map extracted from the full image in **A**. **B, C, D, E** and **F** correspond to the 5th, 7th, 9th, 11th and 13th image of the series. Each image was obtained with an exposure of 18 msec, with a binning of 7 leading to imaes of 59×82 pixels. 25×objective, N.A. 0.6. G: the two upper series of points indicate the fluorescence measured at the two locations indicated by *a* and *b* in **A**. These dots also indicate the timing of image acquisition by the video camera. The cameras shutter remained open for about 20 msec. Lower trace is the electrical signal measured from the connective fibers, following the stimulation of the root

Fig. 8A–D Analysis of the electrical interaction imaged in Fig. 6. **A** and **C** reproduce images obtained as Sp+Sa−Sap where Sp, Sa and Sap are the corresponding images of Fig. 6. Regions in **A** and **C** significantly different from zero indicate non linear interactions between the two inputs delivered to the two roots. **B** and **D** illustrate the analysis of non linear interactions present in **A** and **C**, in yellow saturation, in blue and green shunting inhibition and in red non linear inhibition. The yellow region was obtained as Ba AND Bp and Bap, the green regions as Bp AND (Ba NOR Bap), the blue region as Ba AND (Bp NOR Bap) and the red region as Bp AND Ba (NOT Bap). Binary images Ba, Bp and Bap were obtained from Sa, Sp and Sap by setting a threshold at 1.6‰

Mechanical artifacts

A major problem encountered in this work was the presence of mechanical movement of the preparation induced by the electrical stimulation of the nerves. These movements were not abolished by adding 2.3 butanedione monoxime to the extracellular medium (a compound known to block mechanical contractions in several preparations (Fryer et al. 1988; Györke et al. 1993)), but could be reduced by increasing Mg^{2+} and decreasing Ca^{2+} in the extracellular medium. However, this modification of the level of divalent cations depressed the electrical activity and therefore the signal, too. In order to eliminate these movements, the preparation illustrated in Fig. 1A was used. By tightly sucking the roots and the connective fiber, the three suction electrodes provided a good mechanical stability. The presence of movements of the preparation was checked by displaying the acquired images on the video monitor in rapid succession for visual inspection. A more elaborate way to estimate the presence of mechanical artifacts consisted in the computation of optical flow (De Micheli et al. 1993) from the sequence of fluorescence images. In this way small coherent motions of a pixel fraction could be detected. The presence of movements in the preparation introduced significant artifacts in the image sequences, which could completely mask the real physiological signal. This artifact was usually identified by the appearance of contiguous regions of spurious excitation and inhibition near the moving structure. The image sequences described in this paper were not flawed by the presence of

significant movements of the preparation as checked by visual inspection and by the computation of optical flow. Mechanical artifacts were totally absent when voltage pulses lower than 0.2 V, such as those used in the experiments illustrated in Figs. 4–6, were used to stimulate the ganglion.

Results

As discussed in the Methods section, our imaging system can be used in "real time" mode to detect optical signals larger than 5‰. However, the optical signal measured by our imaging system and generated by the firing of a single action potential is likely to be much smaller than 5‰ and therefore its detection requires the use of the "fixed time" mode. As a consequence, well localized optical signals, presumably produced by the firing of action potentials, were detected in "fixed time" mode. Larger optical signals, produced by the direct polarization of neurons or by a prolonged afterhyperpolarization of after discharge, were measured in "real time" mode.

Imaging the electrical activity in "fixed time" mode

Figure 4D illustrates the electrical signal recorded by a pipette sucking the left posterior root of the ganglion illustrated in A, during the stimulation of the left anterior root with a brief voltage pulse of 0.125 V. This stimulation elicited the discharge of 6 large spikes and possibly some additional spikes of a smaller amplitude. This extracellular voltage response had some variability, but the number of large spikes elicited in different runs was usually the same. By taking fluorescence images at different times it was possible to image the neuronal structures activated during the stimulation of the root and originating the electrical response of Fig. 4D. Signal images taken at different times after the onset of the stimulation are shown in B, C, E and F superimposed to the neuronal map extracted from A with the procedure described in the Methods section (see Fig. 3). The timing of image acquisition is indicated in the upper trace in D.

At the onset of the stimulation the excitation was restricted to the medial N neuron (see Fig. 4B), but rapidly propagated to other neuronal structures: namely the lateral N neuron, the left posterior root and neuronal structures in the middle of the ganglion (see Fig. 4C). At the cessation of the stimulation the electrical activity extinguished within 50 msec, as evident from the electrical response in D and from the signal images in E and F. In this experiment the 5 sensory neurons in the upper left side of the ganglion were well in focus and could be easily recognized and clear optical signals were observed from their cell bodies. Optical signals originating from the posterior root (see panels C, E and F in Fig. 4) were presumably caused by action potentials of neurons with axons in that root. The diffuse optical signal from the middle of the ganglion (see panels C and F of Fig. 4) were likely to be caused by action potentials in interneurons, such as Retzius cells and neurons with neuronal processes in the posterior root and with controlateral processes such as the AP neuron.

Sensory neurons in the leech ganglion have different thresholds and it is therefore interesting to see whether different sensory neurons can be imaged, by changing the strength of the stimulation.

Figure 5, lower row, illustrates electrical signals obtained from the anterior root during the stimulation of the posterior root with brief voltage pulses of progressively larger amplitude. With very weak stimulations no extracellular action potentials were recorded and the measured signal images were within the background noise (data not shown). By increasing the stimulation amplitude, some spikes of a similar shape were elicited (Fig. 5A, B, lower panel). An even larger stimulation caused the appearance of a much larger spike, followed by smaller spikes (Fig. 5D). With a very large voltage step no action potentials were recorded (data not shown). The signal images obtained for the four stimulations are shown in the upper row of Fig. 5. In all signal images a blue-green spot was localized in the posterior root and was most likely caused by the direct polarization of the root with the stimulating hyperpolarizing voltage pulse. Indeed with very large hyperpolarizing voltage pulses (in amplitude larger than 0.2 V) no action potential was elicited and the signal images showed a diffuse and strong hyperpolarization (see Fig. 3D). In this experiment, during a weak stimulation (0.075 V) a clear optical signal was localized over the lateral N neuron (Fig. 5A); with a stronger stimulation a fluorescence change was localized over the medial N neuron. With larger stimulations the optical signal started to invade larger portions of the visible ganglion, as shown in Fig. 5C, D.

These results indicate that different neuronal structures activated by progressively stronger stimulations can be imaged.

Imaging electrical interactions between two different inputs

An important feature of the nervous system is its ability to integrate different stimuli and it is therefore interesting to see whether it is possible to image and to characterize the interaction of two different inputs, such as the stimulation of the left posterior and anterior root of the same ganglion.

The electrical signal evoked by the stimulation of the anterior (posterior) root and recorded from the posterior (anterior) root is reproduced in Fig. 6E. The full image of the ganglion is shown in Fig. 6A. In both cases the electrical stimulation elicited just a few action potentials, presumably produced by different neurons. The first and second rows in Fig. 6 reproduce signal images obtained at the beginning of the stimulation and during the second part of the stimulation, respectively (see shutter artifact in E). Optical signals elicited by the stimulation of the posterior (anterior) left root are shown in the second (third) column and

those elicited by the simultaneous stimulation of both roots are shown in the fourth column. At the beginning of the stimulation optical signals were rather restricted and appeared to be localized to one neuron, which was activated in all signal images in B, C and D. Subsequently the excitation diffused to a larger area of the ganglion. However, the excitation caused by the simultaneous stimulation of both roots (see Fig. 6H) was less diffuse than the excitation induced by the stimulation of just the anterior root (see Fig. 6G). The excitation in images of Fig. 6 extinguished within 60 ms.

Imaging the afterhyperpolarization in real time mode

When hyperpolarizing voltage pulses of a larger amplitude (>0.5 V) were used no action potentials were observed from the roots, but the electrical activity recorded from the connective fiber was clearly modified (see Fig. 1). When large depolarizing voltage pulses were used, a vigorous electrical activity was evoked in the connective fibers. As a consequence it is interesting to establish whether these changes of electrical activity of leech neurons produced optical signals so large as to be also detected in "real time" mode.

Figure 7A illustrates a fluorescence image of another stained leech ganglion. A suction pipette was used to stimulate the posterior left root, which is hardly visible in the fluorescence image shown in Fig. 7A. The stimulation of the root with a large depolarizing voltage (1 V) caused a massive excitation of the ganglion, as indicated by the appearance of a train of action potentials in the connective fibers (see the electrical recording in Fig. 7H). At the cessation of the stimulation the excitation was depressed for some seconds. A good test for our imaging system is to see whether optical signals can be obtained in "real time" mode, localized in time and space, corresponding to the electrical signals measured with the suction pipette (see Fig. 7H).

Figure 7 reproduces signal images S_i obtained during the stimulation of the root sucked into the suction electrode with a depolarizing voltage step. B, C, D, E and F show signal images S_i in false colour (see the scale in the lower left corner) obtained at the 5th, 7th, 9th, 11th and 13th frame of the sequence. These signal images S_i are superimposed on the recovered map of the underlying neuronal structure. A clear, but transient excitation of the root is evident. At the cessation of the direct stimulation, a large and long lasting hyperpolarization could be imaged, most likely caused by an afterhyperpolarization induced by a prolonged membrane depolarization in leech neurons (Baylor & Nicholls 1969; Jansen & Nicholls 1973). The time course of the measured fluorescence at the two locations indicated by a and b in Fig. 7A is reproduced in Fig. 7G. The afterhyperpolarization was completely extinguished within 3 seconds and had the same time course as the depression of the electrical activity observed in the electrical recording to Fig. 7H. The duration of the hyperpolarization described in Fig. 7 increased from about 3 s to about 7 s when other extracellular Ca^{2+} was increased to 15 mM, in agreement with the effect of Ca^{2+} on the afterhyperpolarization in N cells.

In these experiments the optical signal was primarily localized on the anterior left root, which was not directly excited by the suction pipette. When a pair of roots was simultaneously stimulated, optical signals were more diffuse, covering almost half of the ganglion. In other experiments the connective fibers or one or both roots were stimulated and in those cases it was possible to observe signal images of an after discharge. In these experiments the optical signal related to the after discharge was primarily localized on the connective fibers or on the roots.

Discussion

The purpose of this paper was to evaluate the possibility of obtaining fluorescence signals of the electrical activity of neurons in the leech ganglion from fluorescence images acquired with a CCD camera. Our results indicate that fluorescence signals originating from well identified neurons can be obtained and their time course and spatial localization can be resolved with a moderate accuracy. These signal images of the electrical activity can be manipulated in several ways and interesting properties of the neuronal events occurring can be described.

The localization of the optical signal

A good localization of the neuronal structure responsible for the detected optical signal is usually obtained in the presence of a single layer of neurons such as in cultured neurons (Parsons et al. 1991) or in preparations with unusually large neurons such as in the Aplysia (London et al. 1985; Nakashima et al. 1992; Falk et al. 1993; Wu et al. 1994; Tsan et al. 1994). In the presence of a stratified neuronal structure, such as the cortex (Blasdel and Salama 1986) or the olfactory bulb (Kauer 1988) or other olfactory networks (Delaney et al. 1994), the neurons originating the optical signal could not be identified. The present study shows that even in the presence of a multilayered neuronal structure, such as a leech ganglion, it is possible to localize optical signals as originating from identified neurons (see Figs. 3–6). Several factors enhance a good spatial localization: a specific and selective stimulation, a good signal to noise ratio and image processing techniques. The fluorescence images described in this paper were not obtained with a confocal microscope and did not originate from a narrow focal plane. These optical signals were affected by a significant blur in depth. However some experiments indicate that when neurons were not in the focal plane of the microscope, they did not originate a strong fluorescence change. This qualitative observations suggests that the main source of fluorescence changes in the neuronal structure appearing in focus on the microscope objective. The localization of optical signals in the (x, y) plane is satisfactory, being limited by the magnification of

the objective and the binning procedure. The error in the (x, y) plane was of the order of 2 or 3 μM, adequate to localize the cell body of a single neuron.

Temporal resolution

Single action potentials from individual neurons can be well resolved in time by measuring optical signals with photodiodes (Salzberg et al. 1973; Grinvald et al. 1987). A major limitation of using a CCD camera to analyse the electrical activity in the leech nervous system is the reduced time resolution. Our imaging system is able to reliably open and close the shutter within 20 ms, which sets the limit to our time resolution at about 50 Hz. In the "real time" mode images can be acquired at a frame rate of 3–5 Hz, which is adequate only to follow slow electrical signals such as those described in Fig. 7. In the "fixed time" mode and in the presence of a stable preparation, the electrical activity can be sampled at a much higher frequency and our optimal time resolution of 50 Hz can be reached. Our imaging system is not adequate to detect the exact timing of a single spike, but appears to be able to detect the firing of a neuron within a time window of 20 ms (see Figs. 4–6). Given the variability of the firing of leech neurons, it may be convenient to have some temporal smoothing or averaging obtained by integrating signals over a window of 20 ms. The use of specially designed cameras, such as the one recently produced by Fuji (HR Deltaron 1700; see also Tanifuji et al. 1994), can provide a much better temporal resolution, with a satisfactory spatial resolution.

Images of the electrical activity of the leech nervous system

Several physiological properties of the electrical activity of the leech nervous system can be analysed with the optical techniques described in this paper. Firstly, our imaging system is able to follow in "real time" slow electrical signals, such as afterhyperpolarization (Baylor and Nicholls 1969; Jansen and Nicholls 1973) (see Fig. 7). Secondly, in the "fixed time" mode and in the presence of a stable preparation, nonlinear interactions between different inputs can be analysed and a coarse three dimensional description of the electrical activity elicited by a specific stimulation is obtained. The analysis of the interaction between adjacent and distant ganglia with the present technique is likely to be useful for the understanding of neuronal networks controlling swimming (Stent et al. 1978) and crawling (Baader and Kirstan 1995).

Analysis of nonlinear interactions

When reliable images of the electrical activity are obtained, they can be processed so as to gather new and relevant information.

For instance, in order to have a better understanding of the neuronal interactions occurring in the leech ganglia, images shown in Fig. 6 should be analysed in more details. The most evident and straightforward way to analyse the interactions between two different inputs is to verify the degree of linear or nonlinear summation. It is, therefore, convenient to compute the obtained image, I1, as:

$$I1 = (Sa + Sp) - Sap \quad (4)$$

where Sap is the signal image obtained by the simultaneous activation of the left posterior and anterior roots and Sa (Sp) is the signal image obtained by the activation of the anterior (posterior) left root. It is evident that wherever image I1 is close to zero, i.e. within the background noise, the interaction between the two inputs is essentially linear. The image I1, as computed from images of Fig. 6, for the first and second frame is shown in Fig. 8 A and C, respectively. The image in A is almost within the background noise, with the exception of the red-yellow spot localized over a neuron in the upper left side of the ganglion. In contrast, the image in C is significantly different from the background noise in a large portion of the viewed ganglion. As a consequence the interaction between the two inputs was almost linear at the beginning of the stimulation, but became significantly non linear after about 20 ms.

A nonlinear interaction between two inputs may be caused by several mechanisms. An obvious kind of nonlinearity is simply caused by saturation: if both inputs produce the maximal activation of the same neuron, the combination of the two inputs will produce a signal which is less than the sum of the signals produced by the individual inputs. Another kind of nonlinear interaction is caused by shunting or silent inhibition (Torre & Poggio 1978); one input does not cause an appreciable signal, but is able to significantly block the signal produced by the other input.

In order to distinguish between these cases, images should be made binary so that each location of the image is active or silent. Given a threshold τ a binary image B can be obtained by a signal image S, by setting $B_{ij} = 0$ if $S_{ij} < \tau$ and $B_{ij} = 1$ if $S_{ij} > \tau$, where S_{ij} is the image signal at location (i,j). The threshold is set to 1.6‰, i.e. only locations of the image with an optical signal larger than 1.6‰ are considered active. Once images have been made binary it is simple to distinguish between the different cases: saturation occurs at location i,j when the output of the stimulation of each individual roots is 1 and the output of stimulating both roots is again 1. As a consequence, if Ba, Bp and Bap are the binary images of the electrical activity following stimulation of the anterior root, the posterior root and both roots, respectively, the locations on the image where saturation occurs are represented by the binary image Bs:

$$Bs = Ba \text{ AND } Bp \text{ AND } Bap \quad (5)$$

These locations are indicated by the yellow region in the second column of Fig. 8. Similarly locations where the input from the anterior root shunts the excitation elicited by the posterior root can be easily identified as the binary im-

age Bps:

$$Bps = Bp \text{ AND } (Ba \text{ NOR } Bap) \quad (6)$$

where NOR is the AND of the negation of the two binary images. In an analogous way the image Bas, defined as:

$$Bas = Ba \text{ AND } (Bp \text{ NOR } Bap) \quad (7)$$

indicates those locations where stimulation of the anterior root shunts the excitation elicited by the posterior root. Images Bps and Bas are shown as green and blue spots in Fig. 8 B, D respectively.

The interaction between two binary inputs can also be analysed in a more general way. Given two binary inputs, their logical combination may originate 8 possible cases, listed in Table 1 with a conventional definition. The first 3 cases listed in Table 1 can be classified as linear interactions, while the remaining 5 cases are essentially nonlinear interactions, whose saturation and shunting inhibition have already been discussed. Nonlinear inhibition can be detected as the binary image I_{ni}; defined as:

$$I_{ni} = Bp \text{ AND } Ba \text{ AND } (\text{NOT } Bap) \quad (8)$$

and it was also present at some extent in the images shown in Fig. 6. Regions of nonlinear inhibition are indicated in Fig. 8 B, D in red. It may be useful to note that non linearities can be introduced by a larger number of biophysical mechanisms and the classification used in Table 1 and above has to be considered simply as conventional. For instance conduction block (Gu et al. 1989; Gu 1991) is likely to originate many non linear interactions in leech neurons.

It is useful to notice that the neuron in the upper part of the ganglion was characterized by a saturation at the beginning of the stimulation, which became a non linear inhibition after 20 ms.

Superlinearity was almost negligible in images shown in Fig. 6, but was present when each individual input failed to produce any significant signal, but their combination originated an evident optical signal.

The analysis of non linear interactions illustrated in Fig. 8 depends on the threshold used to obtain binary images. When the threshold was varied between 0.9‰ and 2‰ the qualitative analysis of Fig. 8B and D did not change significantly. This simple processing of the signal images of Fig. 6 provides a map of functional interactions between the viewed network and indicates the region of saturation (yellow), of silent inhibition (green and blue) and of nonlinear inhibition (red).

Three dimensional reconstruction of the dynamics of the electrical activity

Once image sequences are available for different focal planes we can recover a three dimensional reconstruction of the dynamics of the electrical activity within the network.

Figure 9 A, B, C and D reproduce four fluorescence images of the ganglion taken by focusing neurons in the most superficial central layer and in other more interior layers.

Table 1 Classification of the interaction between two binary inputs (input 1 and input 2). 8 combinations are possible, three of which can be classified as linear interactions and 5 as nonlinear interactions

Input 1	Input 2	Input 1+2	Interaction
1	0	1	Linear
0	1	1	Linear
0	0	0	Linear
1	1	1	Saturation
1	1	0	Nonlinear inhibition
1	0	0	Shunting inhibition
0	1	0	Shunting inhibition
0	0	1	Superlinearity

Columns indicated by T_1, T_2 and T_3 refer to signal images taken 0, 20 ms and 40 ms after the onset of the stimulation respectively, with T_1 and T_2 during the voltage pulse and T_3 immediately after its cessation. It is evident that a rather weak stimulation of the left posterior root excites several neurons of the ganglion in the ventral layer and in more interior layers.

The width of the ganglion is about 200 μM; for this reason, it was quite difficult to obtain images of the neurons of dorsal layer in focus, when the ventral layer was sitting just above the microscope objectives. Therefore a complete three dimensional reconstruction of the neural activity in a leech ganglion could not be obtained in a single experiment.

CCD cameras vs photodiode arrays

It is evident that photodiode arrays have a temporal resolution adequate to resolve individual action potentials. Commercially available CCD cameras have a limited temporal resolution, but may have a much better spatial resolution. As a consequence the two imaging systems may be advantageous in different cases. It is evident that the optimal imaging system has a good temporal and spatial resolution and these devices may become available in the near future.

Imaging systems generate images, which must be analysed with the most appropriate tools. For instance methods and techniques for image analysis recently developed in Image Resoration, Computer Vision and Graphics could used. This paper presents some simple examples, such as the recovery of the neuronal structure (see Fig. 3), the analysis of nonlinear interactions (see Fig. 8) and of the three dimensional dynamics (see Fig. 9). The development of better imaging systems and appropriate tools for the analysis of these images is likely to provide new and relevant neurobiological insights.

Acknowledgements We are indebted to Drs. Franco Conti, Larry Cohen, Peter Fromherz, Massimo Grattarola, Marco Bove and Maria Teresa Tedesco for many helpful discussions and in particular to Prof. John Nicholls for very valuable suggestions and for reading the manuscript. This work was supported by the EC grant B.R.A. SSS 6961.

References

Baader AP, Kristan WB (1995) Parallel pathways coordinate crawling in the medical leech, Hirudo Medicalis. J Comp Physiol 176:715–726

Baylor DA, Nicholls J (1969) After-effects of nerve impulses on signalling in the central nervous system of the leech. J Physiol 203:571–589

Blasdel GG, Salama G (1986) Voltage-sensitivity dyes reveal a modular organization in monkey striate cortex. Nature 321:579–585

Cohen L, Salzberg MB (1975) Optical measurement of Membrane potential. Rev Physiol Biochem Pharmacol 83:387–410

Delaney KR, Gelperin A, Fee MS, Flore JA, Gervais R, Tank DW, Kleinfeld D (1994) Waves and stimulus-modulated dynamics in an oscillating olfactory network. Proc Natl Acad Sci USA 91:669–673

De Micheli E, Torre V, Uras S (1993) The accuracy of the computation of optical flow and of the recovery of motion parameters. IEEE on PAMI 15:434–447

Falk CX, Wu J-Y, Cohen LB, Tang AC (1993) Nonuniform expression of habituation in the activity of distinct classes of neurons in the aplysia abdominal ganglion. J Neurosci 13:4072–4081

Fryer MW, Neering IR, Stephenson DG (1988) Effects of 2,3-butanedione monoxime on the contractile activation properties of fast and slow twitch rat muscle fibers. J Physiol 407:53–75

Fromherz P, Lambacher A (1991) Spectra of voltage-sensitive fluorescence of styryl-dye in neuron membrane. Biochim Biophys Acta 1068:149–156

Grinvald A (1985) Real-time optical mapping of the neuronal activity: from singlegrowth cones to the intact mammalian brain. Ann Rev Neurosci 8:263–305

Grinvald A, Lieke E, Frostig RD, Gilbert GD, Wiesel TN (1986) Functional architecture of cortex revealed by optical imaging of intrinsic signals. Nature 324:361–363

Grinvald A, Salzberg BM, Lev-Ran V, Hildeshein (1987) Optical recordings of synaptic potentials from processes of single neurons with intracellular potentiometric dyes. Biophys J 51:643–651

Gross GW, Loew LM, Well WW (1986) Optical imaging of cell membrane potential changes induced by applied electric fields. Biophys J 50:339–348

Gu X, Macagno ER, Muller KJ (1989) Laser microbeam axotomy and conduction block show that electrical transmission at a central synapse is distributed at multiple contacts. J Neurobiol 20: 422–434

Gu X (1991) Effect of conduction block at axon bifurcation on synaptic transmission to different postsynaptic neurones in the leech. J Physiol 441:755–778

Györke S, Dettbarn C, Palade P (1993) Potentiation of sarcoplasmic reticulum Ca^{2+} release by 2,3-butanedione monoxime in crustacean muscle. Eur J Physiol 424:39–44

Jansen JKS, Nicholls JG (1973) Conductance changes, an electrogenic pump and the hyperpolarization of leech neurones following impulses. J Physiol 229:636–665

Kauer JS (1988) Real-time imaging of evoked activity in local circuits of salamander olfactory bulb. Nature 331:166-168

London JA, Zecevic D, Cohen LB (1985) Simultaneous monitoring of activity of many neurons from invertebrate ganglia using a multielement detecting system. In: Optical methods in cell physiology. Wiley and Sons, New York

Muller KJ, Nicholls JG, Stent GS (1981) Neurobiology of the leech. Cold Spring Harbor Laboratory, New York

Nakashima M, Yamada S, Shioro S, Maeda M, Satoh F (1992) 448-detector optical recording system: development and applications to Aplysia Gill-Withdrawal reflex. IEEE Trans Biomed Eng 39:26–36

Parsons TD, Salzberg BM, Obaid AL, Raccina-Behling F, Kleinfeld D (1991) Long-term optical recording of patterns of electrical activity in ensembles of cultured aplysia neurons. J Neurophysiol 66:316–333

Salzberg BM, Davila HV, Cohen LB (1973) Optical recordings of impulses in individual neurons of an invertebrate central nervous system. Nature 246:508–509

Stent GS, Kristan WB, Kriesen WO, Ort CA, Poon N, Calabrese RL (1978) Neuronal generation of the leech swimming movement. Science 200:1348–1356

Tanifuji M, Sugiyama T, Murase K (1994) Horizontal propagation of excitation in rat visual cortical slices revealed by optical imaging. Science 266:1057–1058

Torre V, Poggio T (1978) A synaptic mechanism possibly underlying directional selectivity to motion. Proc R Soc Lond B 202:409–416

Tsan Y, Wu JY, Höpp H-P, Cohen LB, Schiminovich P, Falk CX (1994) Distributed aspects of the response to siphon touch in aplysia: spread of stimulus information and cross-correlation analysis. J Neurosci 14:4167–4184

Wu JY, Cohen L (1992) Fast multisite optical measurement of membrane potential fluorescent probes for biological function of living cells. A practical guide. WT Mason, Academic Press

Wu JY, Cohen LB, Falk CX (1994) Neuronal activity during different behaviours in aplysia: a distributed organization. Science 263:820–823